AGU PUBLICATIONS

Geophysical Research Letters

RESEARCH LETTER
10.1002/2014GL062171

Key Points:
- We have obtained a current circuit in the boundary of plasma bubble
- The FACs in the trailing edge of plasma bubble is also region-1-sense
- The current and FACs system is similar to SCW but with much smaller scale

Supporting Information:
- Readme
- Figure S1

Correspondence to:
S. Fu,
suiyanfu@pku.edu.cn

Citation:
Sun, W.-J., S. Fu, Z. Pu, G. K. Parks, J. A. Slavin, Z. Yao, Q.-G. Zong, Q. Shi, D. Zhao, and Y. Cui (2014), The current system associated with the boundary of plasma bubbles, *Geophys. Res. Lett.*, *41*, 8169–8175, doi:10.1002/2014GL062171.

Received 9 OCT 2014
Accepted 6 NOV 2014
Accepted article online 11 NOV 2014
Published online 2 DEC 2014

The current system associated with the boundary of plasma bubbles

Wei-Jie Sun[1,2], Suiyan Fu[1], Zuyin Pu[1], George K. Parks[3], James A. Slavin[2], Zhonghua Yao[4], Qiu-Gang Zong[1], Quanqi Shi[5], Duo Zhao[1], and Yanbo Cui[1]

[1]School of Earth and Space Sciences, Peking University, Beijing, China, [2]Department of Atmospheric, Oceanic and Space Sciences, University of Michigan, Ann Arbor, Michigan, USA, [3]Space Sciences Laboratory, University of California, Berkeley, California, USA, [4]Mullard Space Science Laboratory, University College London, Dorking, UK, [5]Shandong Provincial Key Laboratory of Optical Astronomy and Solar-Terrestrial Environment, School of Space Science and Physics, Shandong University, Weihai, China

Abstract The current system associated with the boundary of plasma bubbles in the Earth's magnetotail has been studied by employing Cluster multipoint observations. We have investigated the currents in both the dipolarization front (DF, leading edge of the plasma bubble) and the trailing edge of the plasma bubble. The distribution of currents at the edge indicates that there is a current circuit in the boundary of a plasma bubble. The field-aligned currents in the trailing edge of the plasma bubble are flowing toward the ionosphere (downward) on the dawnside and away from the ionosphere (upward) on the duskside, in the same sense as region-1 current. Together with previous studies of the current distributions in the DF and magnetic dip region, we have obtained a more complete picture of the current system surrounding the boundary of plasma bubble. This current system is very similar to the substorm current wedge predicted by MHD simulation models but with much smaller scale.

1. Introduction

Bursty bulk flows (BBFs) are one of the most important transient phenomena in the Earth's magnetotail. It has been shown that BBFs transport 60–100% of mass, momentum, and energy of the total plasma sheet transport and therefore play a fundamental role in the magnetospheric activities [*Angelopoulos et al.*, 1992, 1994]. Many investigations have revealed that the braking/diversion of BBFs are highly related with the formation of field-aligned currents (FACs) in the magnetotail [e.g., *Shiokawa et al.*, 1997; *Birn et al.*, 1999; *Slavin et al.*, 2002; *Yao et al.*, 2012]. A plasma bubble [*Pontius and Wolf*, 1990; *Chen and Wolf*, 1993], which is one model of BBF, contains entropy-depleted flux tubes often observed in the magnetotail plasma sheet [e.g., *Sergeev et al.*, 1996; *Wolf et al.*, 2006; *Walsh et al.*, 2009]. In observations, a plasma bubble possesses lower plasma pressure and stronger magnetic field than its ambient plasma. Therefore, the interface between the reconnected flow and background plasma of the plasma sheet is unstable to interchange/ballooning instability and could deform into a wave shape and grows into plasma bubbles in the nonlinear stage [e.g., *Nakamura et al.*, 2002; *Vapirev et al.*, 2013; *Pritchett et al.*, 2014].

The leading edge of the plasma bubble, which is frequently identified as dipolarization front (DF), often exhibits a sharp increase of B_z component of the tail magnetic field accompanied by a decrease of plasma density [see *Sergeev et al.*, 1996; *Runov et al.*, 2009; *Zhou et al.*, 2013; *Liu et al.*, 2014]. A B_z decrease called magnetic dip is frequently observed ahead of the DF [*Ohtani et al.*, 2004; *Runov et al.*, 2009; *Yao et al.*, 2013]. A DF is a structure with spatial scale comparable to the background proton Larmor radius and therefore has strong kinetic properties [*Sergeev et al.*, 2009; *Fu et al.*, 2012; *Huang et al.*, 2012; *Angelopoulos et al.*, 2013]. Recently, a Cluster multipoint study has shown that the normal electric field in the DF layer is mainly contributed by Hall electric field and the duskward electric field by convection electric field. The Hall electric field in the DF layer is in the opposite direction of the magnetic dip region [*Sun et al.*, 2014]. Statistical and case studies revealed that the DF layer current is mainly duskward, and dip current mainly dawnward [*Yao et al.*, 2013; *Liu et al.*, 2013]. The field-aligned component is in the sense of region-1 FAC in the DF layer and, in the dip region, in region-2-sense FAC [*Liu et al.*, 2013; *Sun et al.*, 2013; *Yao et al.*, 2013]. Previous studies have obtained currents associated with DF and the magnetic dip region. But it is still not clear about the current in the trailing edge of plasma bubble.

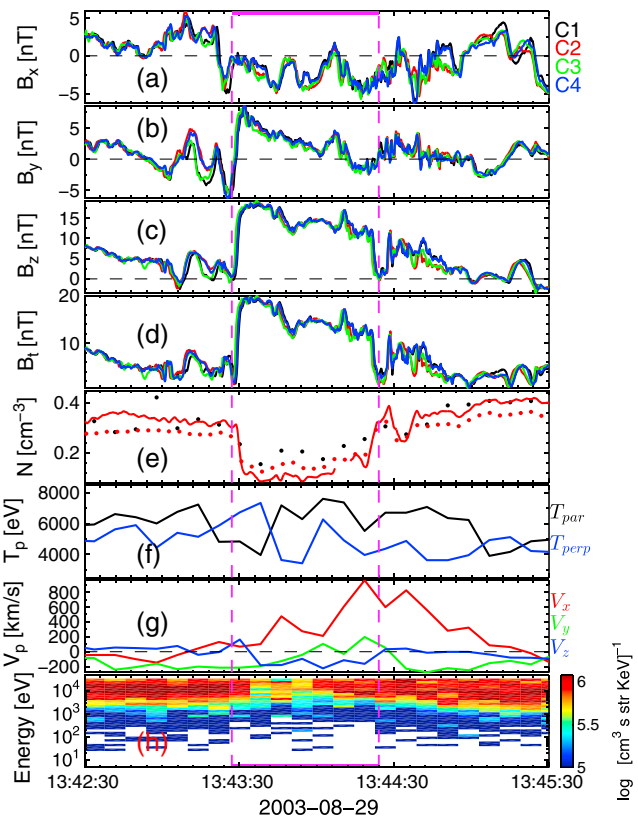

Figure 1. (a) B_x, (b) B_y, (c) B_z, and (d) B_t. (e) Plasma density. Black dots represent the proton density; red dots represent the electron density from C2 PEACE, and red line represents the electron density deduced from C2 spacecraft potential [*Pedersen et al.*, 2008]. (f) Proton parallel (T_{par}, black) and perpendicular (T_{perp}, blue) temperatures, (g) proton bulk velocity V_x (red), V_y (green), and V_z (blue), and (h) energy spectrum for proton differential particle flux. Proton data are from C1 CIS-CODIF. The four spacecraft in Figures 1a to 1d are color coded. Plasma bubble is defined between the two vertical dashed lines.

In this paper, by employing the Cluster data, we will investigate the currents associated with DF as well as the trailing edge of the plasma bubble to obtain a more complete picture of current system associated with the boundary of a plasma bubble. In the 2003 tail season the separations among Cluster satellites were ~ 100–300 km, enabling the application of multispacecraft methods on subproton spatial scales (~ 1000 km). The results show that there is current flowing in the boundary of plasma bubble, which partially closes in the boundary and the ionosphere via region-1-sense FAC.

2. Observations

The magnetic field (22.4 samples per second), ion, electron, and spacecraft potential (five samples per second) data used in this study come from the experiments on Cluster: Fluxgate Magnetometer (FGM) [*Balogh et al.*, 2001], Cluster Ion Spectrometry (CIS) [*Rème et al.*, 2001], Plasma Electron And Current Experiment (PEACE) [*Johnstone et al.*, 1997], and Electric Field and Wave (EFW) [*Gustafsson et al.*, 2001].

2.1. Case Study

Figure 1 shows the event overview made by Cluster between 1342:30 and 1345:30 UT on 29 August 2003. Cluster was located at [−17.53, −1.85, 2.77] R_E. All quantities in this study are in Geocentric Solar Magnetospheric (GSM) coordinates unless otherwise indicated. During this time interval, $|B_x| < 5$ nT (Figure 1a), plasma density $n_p < 0.4$ cm^{-3} (Figure 1e), and proton temperature $k_B T_p \sim 5$ keV (Figure 1f) are consistent with those of plasma sheet. A plasma bubble is defined between the two dashed lines with stronger magnetic field (Figure 1d) and lower plasma density (Figure 1e) than the ambient plasma, which is also accompanied with high-speed earthward flow, $v_{x,max} > 800$ km/s (Figure 1g). The ion temperature is almost unchanged during this time interval. Plasma beta (β) of the ambient plasma is estimated to be ~25, which confirms the satellite being in the inner plasma sheet [*Angelopoulos et al.*, 1994]. The leading edge of this plasma bubble is a well-defined DF observed at ~ 1343:30, which was accompanied by a sharp increase of B_z (from ~ 0 to ~ 15 nT in 5 s) and decrease of n_p (from ~ 0.3 to ~ 0.1 cm^{-3}). The trailing edge of the plasma bubble is identified by a sharp decrease of B_z (from ~ 10 to ~ 0 nT in 3 s) and increase of n_p (from ~ 0.15 to ~ 0.3 cm^{-3}) at ~ 1344:20 UT. It is worth noticing that there is a small plasma bubble with intense magnetic field behind this event, which also corresponds to a decrease of plasma density and high-speed plasma flow.

Figure 2 shows observations of the current density at the DF and the trailing edge of the plasma bubble shown in Figure 1. During this time interval, Cluster formed a regular tetrahedron configuration: the elongation and planarity of the four spacecraft tetrahedron were 0.22 and 0.25. Thus, the curlometer technique can be used to calculate the current density [*Robert et al.*, 1998]. The magnitude of $|\nabla \cdot \mathbf{B}/\nabla \times \mathbf{B}|$, which gives an estimate of the error of current density calculation, is smaller than 0.3 around the DF layer and trailing edge, affirming that the curlometer calculation is reliable [*Robert et al.*, 1998]. The normal directions of the DF and trailing edge were [0.7, −0.61, 0.37] and [0.61, −0.79, 0.02], respectively. The Minimum Variance

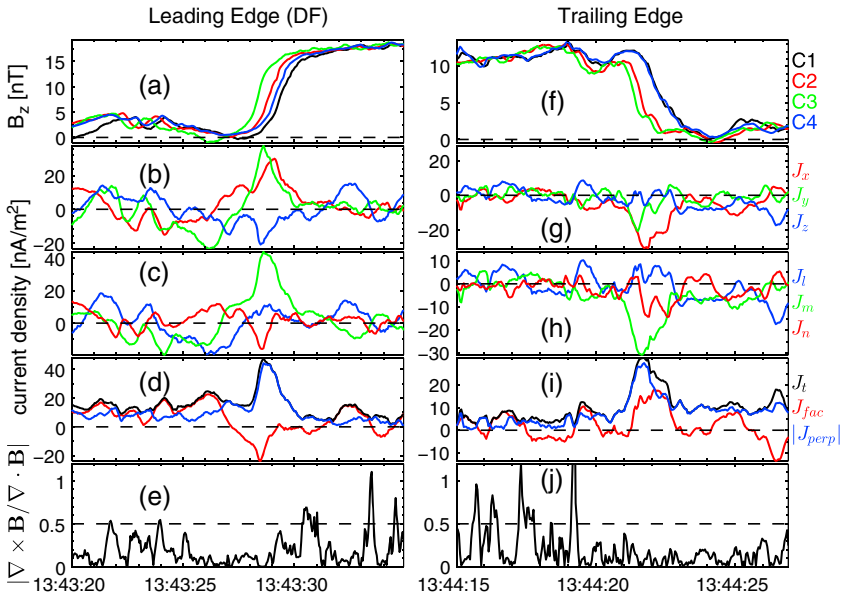

Figure 2. (a, f) B_z. (b, g) Current density components in *GSM* coordinate, J_x (red), J_y (green), and J_z (blue). (c, h) Current density components in *LMN* coordinate, J_l (blue), J_m (green), and J_n (red). (d, i) Total current density (J_t, black), field aligned (J_{fac}, red), and magnitude of perpendicular ($|J_{perp}|$, blue) components. (e, j) Magnitude of $|\nabla \cdot \mathbf{B}/\nabla \times \mathbf{B}|$.

Analysis (MVA) [*Sonnerup and Cahill*, 1967] eigenvalue ratio ($\lambda_2 / \lambda_3 > 10$) is large enough to ensure that the calculation of minimum variance directions is reliable. We have deduced that Cluster crossed the dawnside of the DF and duskside of the trailing edge since the shape of plasma bubble in the *XY* plane is similar to an ellipse [*Chen and Wolf*, 1993; *Liu et al.*, 2014]. The current in the DF layer is flowing earthward and duskward (Figure 2b), which is opposite to that in the trailing edge that flows in tailward and dawnward direction (Figure 2g). We have adopted the *LMN* coordinate system obtained from MVA analysis to further investigate the properties of the current in the layers. We let **n** be sunward, **l** northward, and $\mathbf{m} = -\mathbf{n} \times \mathbf{l}$ (duskward) in this study, the same definition that was applied previously in *Yao et al.* [2013]. The current is dominated by $J_m(-J_m)$ in the DF layer (trailing edge) as shown in Figure 2c (Figure 2h), and this current is mainly at the boundary of the plasma bubble. Therefore, we see that the currents of DF and trailing edge are in opposite local directions. Because Cluster crossed the dawnside of DF layer and duskside of trailing edge, the observations suggest a closed current circuit around the plasma bubble boundary. The estimate of averaged perpendicular current density in the DF layer is ~ 27.1 nA/m^2 and ~ 19.8 nA/m^2 in the trailing edge, indicating that most of the DF layer current is closed via the trailing edge of this plasma bubble. These currents will be studied further in the following section.

Both of the DF and trailing edge were observed in the Southern Hemisphere with negative B_x (Figure 1a). A magnetic dip region is identified ahead of the DF with B_z decrease ~ 5 nT in ~ 4 *s* [e.g., *Yao et al.*, 2013]. The FAC is parallel to the magnetic field (upward from the ionosphere) in the magnetic dip region (ahead of the DF) and antiparallel to the magnetic field (downward to the ionosphere) in the DF layer (Figure 2d). Because Cluster crossed the dawnside of the DF, these FACs are consistent with previous results that region-1-sense FACs flow inside the DF layer and region-2-sense FACs flow in the magnetic dip region [*Liu et al.*, 2013; *Sun et al.*, 2013; *Yao et al.*, 2013]. When Cluster crossed the duskside of the trailing edge, the FAC is parallel to the magnetic field (upward from the ionosphere) as shown in Figure 2i, which is a region-1-sense FAC.

2.2. Statistical Study

The case study reveals that the current could be closed around the boundary of plasma bubble and that the FAC in the trailing edge is similar to region-1-sense current. A statistical study is now performed to confirm these results. Based on the DF list of *Yao et al.* [2013], we have further selected plasma bubbles based on the following criteria: (1) the event accompanied earthward plasma flow with total velocity (v_t) is higher than 300 km/s, (2) the event contains a lower plasma density and stronger magnetic field than the background plasma sheet, which is in front of the compression region, and (3) the DF and trailing edge is well defined; i.e., the DF corresponds to the increase of magnetic field intensity and decrease of plasma density, and the

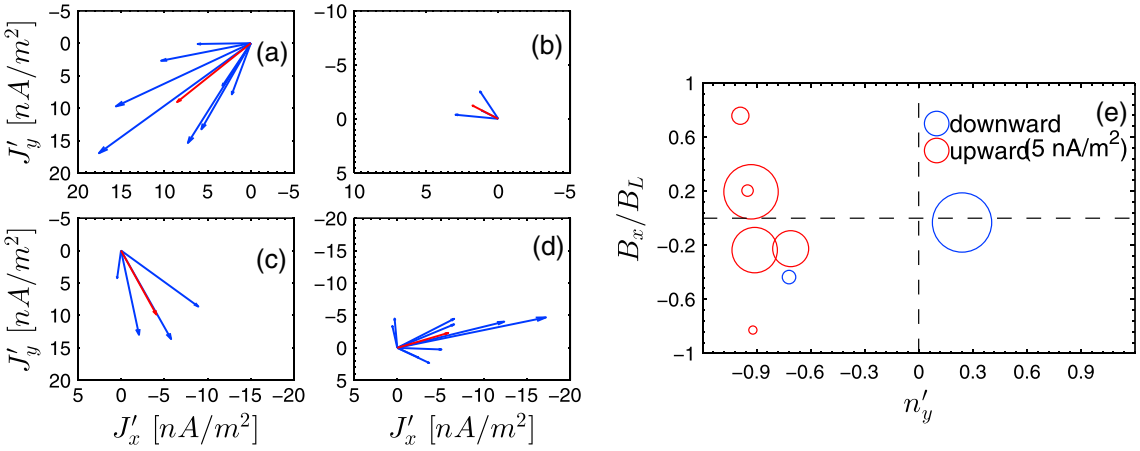

Figure 3. Current density distribution of the 12 plasma bubbles boundaries in the *XY* plane, which has been divided into four regions according to their n'_y: (a) the crossings of DF with $n'_y < 0$, (b) the crossings of trailing edge with $n'_y > 0$, (c) the crossings of DF with $n'_y > 0$, and (d) the crossings of trailing edge with $n'_y < 0$. (e) The FACs in the trailing edge. B_x/B_L is an estimation of the distance from neutral sheet, and n'_y denote the crossing direction of the spacecraft relative to the trailing edges. Currents flowing toward the ionosphere are shown as blue circles and those out of the ionosphere as red circles. The size of the circle denotes the averaged intensity of the FAC.

trailing edge corresponds to the decrease of magnetic field intensity and increase of plasma density. Using these selection criteria resulted in 12 plasma bubbles.

First, we will determine the relative normal direction and current density since the plasma bubbles are not always moving along the *X* direction. The moving direction of plasma bubble is estimated from the observed plasma flow. The relative normal direction (n') and current density (J') are obtained according to this direction as we have deduced that this direction is X'. In the case study section, we showed that the plasma bubble moving direction is [0.95, −0.07, −0.30] (normalized from plasma flow: [386, −43, −113] km/s, which is from CIS-CODIF of C1; the observation from C4 is similar), which has a small n_y. Therefore, the n and J of this event is almost the same as n' and J'. We want to note that, though a v_y reverse in the middle of plasma bubble, the integrated moving distance of this plasma bubble in $-Y$ direction (dawnward) is $\sim 0.36\ R_E$, indicating that the dawnside crossing of DF and duskside crossing of trailing edge is reasonable. Furthermore, we divide the boundaries of plasma bubbles into four regions/groups according to n' and show their current (J') distribution in this four regions shown in Figures 3a to 3d. Figure 3a (Figure 3c) is for the dawnside (duskside) crossings of DF with $n'_y < 0$ (> 0), and Figure 3b (Figure 3d) is the dawnside (duskside) crossings of trailing edge with $n'_y > 0$ (< 0). The blue arrows denote the current measurements of each crossing, and the red arrow in each figure is the averaged current density of each region. We can see that the current is earthward and duskward in the dawnside of the DF and tailward and duskward in the duskside of the DF, while they are tailward and dawnward in the duskside of the trailing edge and earthward and dawnward in the dawnside of the trailing edge. This statistical result further indicates that there is a current circulating around the boundary of the plasma bubbles.

The superposed analysis (see the supporting information) of the 12 plasma bubbles shows that the averaged current density of the DF is larger than that of the trailing edge, but about half of the current is field-aligned, which connects to the ionosphere. While the field-aligned component of the trailing edge is smaller than the perpendicular component, our results show that most of the perpendicular current in the DF is closed with the trailing edge, which supports the results of the case study.

In order to determine the properties of FACs in the trailing edge, we have also selected the trailing edges to the south and north of the neutral sheet. This has resulted in 8 of the 12 events. Figure 3e shows the FACs in the trailing edge. The ratio B_x/B_L estimates the distance of the satellite to the neutral sheet, where B_L is the magnitude of lobe field and n'_y indicates the crossing direction of the satellite relative to the trailing edge. The B_L is deduced from the pressure balance between the plasma sheet and lobe

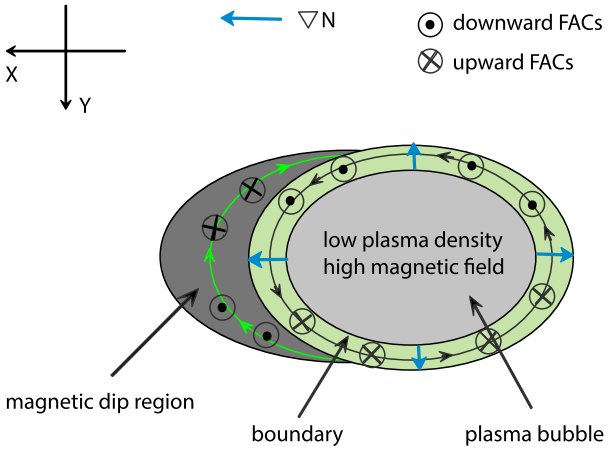

Figure 4. A schematic to illustrate the current associated with the plasma bubble in GSM *XY* plane. Magnetic dip region is plotted as shaded black region earthward of the plasma bubble. The shaded gray elliptical region indicates the plasma bubble, and the shaded green region represents the boundary of plasma bubble.

[see, *Liu et al.*, 2013; *Sun et al.*, 2013]. Figure 3e shows that the FACs are flowing downward into the ionosphere on the dawnside and upward out of the ionosphere on the duskside for the trailing edges, which are a current in the region-1-sense. These results agree with the previous results that show that the FACs in the DF are also in the region-1-sense [*Sun et al.*, 2013]. Thus, we can conclude that the FACs in the boundary of plasma bubbles are in the region-1-sense.

3. Summary and Discussion

In this paper, we used Cluster observations and studied the currents around the boundary of plasma bubbles. We have not only studied the DF (usually on the leading edge of plasma bubbles) but also the trailing edge of plasma bubble. Together with the results from previous studies on the currents in the DF and magnetic dip region [*Liu et al.*, 2013; *Sun et al.*, 2013; *Yao et al.*, 2013], we have now obtained a more complete picture of the current system associated with the boundary of plasma bubbles. A summary of this current system is schematically shown in Figure 4. This figure is in the *XY* plane. The plasma bubble is represented by the shaded gray elliptical region, and the magnetic dip region is indicated by the shaded black region earthward of the plasma bubble. From this figure, we can see that there is a closed current system around the boundary of plasma bubbles (shaded green region around the plasma bubble in Figure 4). The current flows in the anticlockwise sense and also have field-aligned components above and below the neutral sheet. The FACs are flowing toward the ionosphere (downward) on the plasma bubbles dawnside and away from the ionosphere (upward) on the duskside, which is in the sense of the region-1 current. In the magnetic dip region, FACs are downward in the duskside and upward in the dawnside, which is in the direction of the region-2-sense. These currents are the main components of the dawnward currents in the magnetic dip region [*Yao et al.*, 2013]. As proposed by *Yao et al.* [2013], a part of the DF layer current could be closed via the current in the dip region. Our estimation reveals that the total perpendicular current in the trailing edge is slightly smaller than the DF layer, indicating that only a small part of the DF layer current flows in the dip region. This current system is similar with that of the substorm current wedge (SCW) in MHD simulation [*Birn and Hesse*, 2014, Figure 5; see also *Birn and Hesse*, 2013; *Kepko et al.*, 2014]. The flow shears driven by earthward movement of plasma bubble could also generate region-1-sense FACs around the plasma bubble [*Birn et al.*, 2004; *Takada et al.*, 2008; *Walsh et al.*, 2009]. But we have to note that the scale of flow shear driving FACs and SCW could be several Earth radii [e.g., *Walsh et al.*, 2009; *Yao et al.*, 2012]. The current of the current system in this study mainly exists in the boundary of plasma bubble with scale of $\sim$ 1000 km. The average scale of the plasma bubbles is estimated to be $\sim$ 1.5 R_E, which indicates that the circuit of the boundary current could be comparable with the SCW. Previous studies showed that DF-related streamers in the expansion phase of substorm could abruptly contribute to the ground magnetic field disturbance [*Lyons et al.*, 2012]. And plasma bubble-associated streamers could lead to substorm onset [*Nishimura et al.*, 2010]. But whether the streamer is associated with this current system is not known. The geomagnetic effect of this current system also desires further study.

The shape of plasma bubble may not be a simple elliptical shape in the *XY* plane as we plotted in Figure 4. But with the assumption that $n'_y < 0$ and $n'_y > 0$ corresponds with the duskside and dawnside of trailing edge, we have obtained the region-1-sense FACs in the trailing edge. This is in the same sense with that of MHD simulations [*Birn and Hesse*, 2013, 2014] and observations [*Takada et al.*, 2008; *Walsh et al.*, 2009], which indicate that this assumption is applicable. The shape of plasma bubble is certainly needed to be further studied. *Mostl et al.* [2009] applied the Grad-Shafranov Reconstruction on magnetic cloud structure and

obtained the current distribution of it without assuming the shape of magnetic cloud. The application of this technique on the plasma bubble might be useful and is needed for further investigation.

The outflow of reconnected lobe plasma from the reconnection site is the likely cause of the reduction of the density inside the bubble as compared to the background plasma. Thus, there exists a strong plasma density gradient at the boundary, which is represented by the blue arrows in Figure 4. Because the magnetic field is pointing northward, the diamagnetic current ($\mathbf{J} = \mathbf{B}/B^2 \times \nabla P$) caused by this density gradient is in the same sense with our observation of perpendicular current in the boundary. Another possible contributor is the inertial current ($-\rho d\mathbf{v}/dt \times \mathbf{B}/B^2$), but previous study showed that it is very small in comparison with diamagnetic current and often ignored even in the near-Earth region [*Keiling et al.*, 2009; *Yao et al.*, 2012]. Our events are located farther downtail ($< -15\ R_E$) and contain much lower plasma density compared with the background. It is reasonable to ignore the inertial current in this study. We therefore suggest that the perpendicular current in the boundary could be at least part of the diamagnetic current. The anticlockwise flowing boundary current would generate northward magnetic field according to Ampere's law. This picture is supported by the higher intensity of magnetic field inside the plasma bubble, which is consistent with *Birn and Hesse* [2014, Figure 6b].

As shown in previous studies, B_z gradually decreases to the undisturbed value after the crossing of DF [*Runov et al.*, 2011]. In our case observation, strong B_z inside the plasma bubble persisted for $\sim$ 50 s and then decreased to approximately the initial value identified as the trailing edge and also shown in *Zhou et al.* [2013]. Most of the plasma bubbles show that the DFs and trailing edges have comparable scales and the same magnitude of the current density. But in some plasma bubbles (3/12) we studied, the thickness of the trailing edge is $\sim$2 times the DF and the current density in the trailing edge has smaller intensity than observed in the DFs. These observations indicate that the current in the trailing edge exists in a wider region with smaller density in some plasma bubbles than in others. The difference between the two kinds of plasma bubbles suggests they might be at different stages of development. Further studies will consider how the evolution of plasma bubble and the boundaries in the magnetotail evolve in space and time.

Acknowledgments

The data used in this study were obtained from Cluster Active Archive (CAA) (http://caa.estec.esa.int/), which is available to the worldwide scientific community. We are grateful to Cluster FGM, CIS, PEACE, EFW teams, and CAA for providing the high-quality data. Wei-Jie Sun thanks Jiang Liu, Xiaoyan Zhou (UCLA, U.S.), and Xuzhi Zhou (Peking University, China) for helpful discussions. This work is supported by the National Nature Science Foundation of China (grants 41474139, 41031065, 41274167, and 41322031) and partly supported by Chinese Key Research Project (2011CB811404). Wei-Jie Sun is supported by the State Scholarship Fund of Chinese Scholarship Council for his study in AOSS, University of Michigan, Ann Arbor.

W. K. Peterson thanks two anonymous reviewers for their assistance in evaluating this paper.

References

Angelopoulos, V., W. Baumjohann, C. F. Kennel, F. V. Coroniti, M. G. Kivelson, R. Pellat, R. J. Walker, H. Lühr, and G. Paschmann (1992), Bursty bulk flows in the inner central plasma sheet, *J. Geophys. Res.*, *97*, 4027–4039.

Angelopoulos, V., C. F. Kennel, F. V. Coroniti, R. Pellat, M. G. Kivelson, R. J. Walker, C. T. Russell, W. Baumjohann, W. C. Feldman, and J. T. Gosling (1994), Statistical characteristics of bursty bulk flow events, *J. Geophys. Res.*, *99*, 21,257–21,280.

Angelopoulos, V., A. Runov, X.-Z. Zhou, D. L. Turner, S. A. Kiehas, S.-S. Li, and I. Shinohara (2013), Electromagnetic energy conversion at reconnection fronts, *Science*, *341*(6153), 1478–1482, doi:10.1126/science.1236992.

Balogh, A., et al. (2001), The Cluster magnetic field investigation: Overview of in-flight performance and initial results, *Ann. Geophys.*, *19*(10–12), 1207–1217, doi:10.5194/angeo-19-1207-2001.

Birn, J., and M. Hesse (2013), The substorm current wedge in MHD simulations, *J. Geophys. Res. Space Physics*, *118*, 3364–3376, doi:10.1002/jgra.50187.

Birn, J., and M. Hesse (2014), The substorm current wedge: Further insights from MHD simulations, *J. Geophys. Res. Space Physics*, *119*, 3503–3513, doi:10.1002/2014JA019863.

Birn, J., M. Hesse, G. Haerendel, W. Baumjohann, and K. Shiokawa (1999), Flow braking and the substorm current wedge, *J. Geophys. Res.*, *104*(A9), 19,895–19,903, doi:10.1029/1999JA900173.

Birn, J., J. Raeder, Y. L. Wang, R. A. Wolf, and M. Hesse (2004), On the propagation of bubbles in the geomagnetic tail, *Ann. Geophys.*, *22*(5), 1773–1786.

Chen, C. X., and R. A. Wolf (1993), Interpretation of high-speed flows in the plasma sheet, *J. Geophys. Res.*, *98*, 21,409–21,419.

Fu, H. S., Y. V. Khotyaintsev, A. Vaivads, M. André, and S. Y. Huang (2012), Electric structure of dipolarization front at sub-proton scale, *Geophys. Res. Lett.*, *39*, L06105, doi:10.1029/2012GL051274.

Gustafsson, G., et al. (2001), First results of electric field and density observations by CLUSTER EFW based on initial months of operation, *Ann. Geophys.*, *19*, 1219–1240.

Huang, S. Y., et al. (2012), Kinetic structure and wave properties associated with sharp dipolarization front observed by cluster, *Ann. Geophys.*, *30*, 97–107, doi:10.5194/angeo-30-97-2012.

Johnstone, A. D., et al. (1997), PEACE: A plasma electron and current experiment, *Space Sci. Rev.*, *79*, 351–398.

Keiling, A., et al. (2009), Substorm current wedge driven by plasma flow vortices: THEMIS observations, *J. Geophys. Res.*, *114*, A00C22, doi:10.1029/2009JA014114.

Kepko, E. L., K.-H. Glassmeier, J. Slavin, and T. Sundberg (2014), The substorm current wedge at Earth and Mercury, in *AGU Monograph, Magnetotails in the Solar System*, edited by A. Keiling, C. Jackman, and P. Delamere, chap. 21, AGU, Washington, D. C., in press.

Liu, J., V. Angelopoulos, A. Runov, and X.-Z. Zhou (2013), On the current sheets surrounding dipolarizing flux bundles in the magnetotail: The case for wedgelets, *J. Geophys. Res. Space Physics*, *118*, 2000–2020, doi:10.1002/jgra.50092.

Liu, J., V. Angelopoulos, X.-Z. Zhou, and A. Runov (2014), Magnetic flux transport by dipolarizing flux bundles, *J. Geophys. Res. Space Physics*, *119*, 909–926, doi:10.1002/2013JA019395.

Lyons, L. R., Y. Nishimura, X. Xing, A. Runov, V. Angelopoulos, E. Donovan, and T. Kikuchi (2012), Coupling of dipolarization front flow bursts to substorm expansion phase phenomena within the magnetosphere and ionosphere, *J. Geophys. Res.*, *117*, A02212, doi:10.1029/2011JA017265.

Mostl, C., C. Farrugia, H. Biernat, M. Leitner, E. Kilpua, A. Galvin, and J. Luhmann (2009), Optimized Grad-Shafranov reconstruction of a magnetic cloud using stereo-wind observations, *Sol. Phys.*, *256*(1–2), 427–441, doi:10.1007/s11207-009-9360-7.

Nakamura, M. S., H. Matsumoto, and M. Fujimoto (2002), Interchange instability at the leading part of reconnection jets, *Geophys. Res. Lett.*, *29*(8), 88–1–88–4, doi:10.1029/2001GL013780.

Nishimura, Y., L. Lyons, S. Zou, V. Angelopoulos, and S. Mende (2010), Substorm triggering by new plasma intrusion: THEMIS all-sky imager observations, *J. Geophys. Res.*, *115*, A07222, doi:10.1029/2009JA015166.

Ohtani, S.-I., M. A. Shay, and T. Mukai (2004), Temporal structure of the fast convective flow in the plasma sheet: Comparison between observations and two-fluid simulations, *J. Geophys. Res.*, *109*, A03210, doi:10.1029/2003JA010002.

Pedersen, A., et al. (2008), Electron density estimations derived from spacecraft potential measurements on Cluster in tenuous plasma regions, *J. Geophys. Res.*, *113*, A07S33, doi:10.1029/2007JA012636.

Pontius, D. H., Jr., and R. A. Wolf (1990), Transient flux tubes in the terrestrial magnetosphere, *Geophys. Res. Lett.*, *17*, 49–52.

Pritchett, P. L., F. V. Coroniti, and Y. Nishimura (2014), The kinetic ballooning/interchange instability as a source of dipolarization fronts and auroral streamers, *J. Geophys. Res. Space Physics*, *119*, 4723–4739, doi:10.1002/2014JA019890.

Rème, H., et al. (2001), First multispacecraft ion measurements in and near the Earth's magnetosphere with the identical Cluster ion spectrometry (CIS) experiment, *Ann. Geophys.*, *19*(10–12), 1303–1354, doi:10.5194/angeo-19-1303-2001.

Robert, P., M. W. Dunlop, A. Roux, and G. Chanteur (1998), Accuracy of current density determination, in *Analysis Methods for Multi-Spacecraft Data*, edited by G. Paschmann and P. W. Daly, chap. 16, pp. 395–418, ISSI/ESA, Netherlands.

Runov, A., V. Angelopoulos, M. I. Sitnov, V. A. Sergeev, J. Bonnell, J. P. McFadden, D. Larson, K.-H. Glassmeier, and U. Auster (2009), THEMIS observations of an earthward-propagating dipolarization front, *Geophys. Res. Lett.*, *36*, L14106, doi:10.1029/2009GL038980.

Runov, A., V. Angelopoulos, X.-Z. Zhou, X.-J. Zhang, S. Li, F. Plaschke, and J. Bonnell (2011), A THEMIS multicase study of dipolarization fronts in the magnetotail plasma sheet, *J. Geophys. Res.*, *116*, A05216, doi:10.1029/2010JA016316.

Sergeev, V., V. Angelopoulos, S. Apatenkov, J. Bonnell, R. Ergun, R. Nakamura, J. McFadden, D. Larson, and A. Runov (2009), Kinetic structure of the sharp injection/dipolarization front in the flow-braking region, *Geophys. Res. Lett.*, *36*(21), L21105, doi:10.1029/2009GL040658.

Sergeev, V. A., V. Angelopoulos, J. T. Gosling, C. A. Cattell, and C. T. Russell (1996), Detection of localized, plasma-depleted flux tubes or bubbles in the midtail plasma sheet, *J. Geophys. Res.*, *101*, 10,817–10,826.

Shiokawa, K., W. Baumjohann, and G. Haerendel (1997), Braking of high-speed flows in the near-Earth tail, *Geophys. Res. Lett.*, *24*, 1179–1182.

Slavin, J. A., et al. (2002), Simultaneous observations of earthward flow bursts and plasmoid ejection during magnetospheric substorms, *J. Geophys. Res.*, *107*(A7), 1106, doi:10.1029/2000JA003501.

Sonnerup, B. U. O., and L. J. Cahill (1967), Magnetopause structure and attitude from Explorer 12 observations, *J. Geophys. Res.*, *72*, 171–183.

Sun, W. J., S. Y. Fu, G. K. Parks, J. Liu, Z. H. Yao, Q. Q. Shi, Q.-G. Zong, S. Y. Huang, Z. Y. Pu, and T. Xiao (2013), Field-aligned currents associated with dipolarization fronts, *Geophys. Res. Lett.*, *40*, 4503–4508, doi:10.1002/grl.50902.

Sun, W.-J., S. Fu, G. K. Parks, Z. Pu, Q.-G. Zong, J. Liu, Z. Yao, H. Fu, and Q. Shi (2014), Electric fields associated with dipolarization fronts, *J. Geophys. Rese. Space Physics*, *119*, 5272–5278, doi:10.1002/2014JA020045.

Takada, T., et al. (2008), Local field-aligned currents in the magnetotail and ionosphere as observed by a Cluster, Double Star, and MIRACLE conjunction, *J. Geophys. Res.*, *113*, A07S20, doi:10.1029/2007JA012759.

Vapirev, A., G. Lapenta, A. Divin, S. Markidis, P. Henri, M. Goldman, and D. Newman (2013), Formation of a transient front structure near reconnection point in 3-D PIC simulations, *J. Geophys. Res. Space Physics*, *118*, 1435–1449, doi:10.1002/jgra.50136.

Walsh, A. P., et al. (2009), Cluster and Double Star multipoint observations of a plasma bubble, *Ann. Geophys.*, *27*(2), 725–743, doi:10.5194/angeo-27-725-2009.

Wolf, R. A., V. Kumar, F. R. Toffoletto, G. M. Erickson, A. M. Savoie, C. X. Chen, and C. L. Lemon (2006), Estimating local plasma sheet PV5/3 from single-spacecraft measurements, *J. Geophys. Res.*, *111*, A12218, doi:10.1029/2006JA012010.

Yao, Z., et al. (2013), Current structures associated with dipolarization fronts, *J. Geophys. Res. Space Physics*, *118*, 6980–6985, doi:10.1002/2013JA019290.

Yao, Z. H., et al. (2012), Mechanism of substorm current wedge formation: THEMIS observations, *Geophys. Res. Lett.*, *39*, L13102, doi:10.1029/2012GL052055.

Zhou, M., X. H. Deng, M. Ashour-Abdalla, R. J. Walker, Y. Pang, C. Tang, M. El-Alaoui, Z. G. Yuan, and H. M. Li (2013), Cluster observations of kinetic structures and electron acceleration within a dynamic plasma bubble, *J. Geophys. Res. Space Physics*, *118*, 674–684, doi:10.1029/2012JA018323.